Contrib Mineral Petrol (2006) 151: 158–173
DOI 10.1007/s00410-005-0052-5

ORIGINAL PAPER

Andrea De Stefano · Nathalie Lefebvre · Maya Kopylova

Enigmatic diamonds in Archean calc-alkaline lamprophyres of Wawa, southern Ontario, Canada

Received: 31 March 2005 / Accepted: 10 November 2005 / Published online: 5 January 2006

Abstract A suite of 80 macrodiamonds recovered from volcaniclastic breccia of Wawa (southern Ontario) was characterized on the basis of morphology, nitrogen content and aggregation, cathodoluminescence (CL), and mineral inclusions. The host calc-alkaline lamprophyric breccias were emplaced at 2.68–2.74 Ga, contemporaneously with voluminous bimodal volcanism of the Michipicoten greenstone belt. The studied suite of diamonds differs from the vast majority of diamond suites found worldwide. First, the suite is hosted by calc-alkaline lamprophyric volcanics rather than by kimberlite or lamproite. Second, the host volcanic rock is amongst the oldest known diamondiferous rocks on Earth, and has experienced regional metamorphism and deformation. Finally, most diamonds show yellow-orange-red CL and contain mineral inclusions not in equilibrium with each other or their host diamond. The majority of the diamonds in the Wawa suite are colorless, weakly resorbed, octahedral single crystals and aggregates. The diamonds contain 0–740 ppm N and show two modes of N aggregation at 0–30 and 60–95% B-centers suggesting mantle storage at 1,100–1,170°C. Cathodoluminescence and FTIR spectroscopy shows that emission peaks present in orange CL stones do not likely result from irradiation or single substitutional N, in contrast to other diamonds with red CL. The diamonds contain primary inclusions of olivine (Fo_{92} and Fo_{89}), omphacite, orthopyroxene (En_{93}), pentlandite, albite, and An-rich plagioclase. These peridotitic and eclogitic minerals are commonly found within single diamonds in a mixed paragenesis which also combines shallow and deep phases. This apparent disequilibrium can be explained by effective small-scale mixing of subducted oceanic crust and mantle rocks in fast "cold" plumes ascending from the top of the slabs in convergent margins. Alternatively, the diamonds could have formed in the pre-2.7–2.9 Ga cratonic mantle and experienced subsequent alteration of syngenetic inclusions related to host magmatism and ensuing metamorphism. Neither orogenic nor cratonic model of the diamond origin fully explains all of the observed characteristics of the diamonds and their host rocks.

Electronic Supplementary Material Supplementary material is available for this article at http://dx.doi.org/10.1007/s00410-005-0052-5 and is accessible for authorized users.

Communicated by T. L. Grove

A. De Stefano (✉) · M. Kopylova
Department of Earth and Ocean Sciences,
University of British Columbia, 6339 Stores Rd,
V6T 1Z4 Vancouver, Canada
E-mail: adestefano@eos.ubc.ca
Tel.: +1-604-8220671
Fax: +1-604-8226088

Present address: N. Lefebvre
De Beers Canada Exploration, 1 William Morgan Drive,
M4H 1N6 Toronto, ON, Canada

Introduction

Diamond, like all other minerals, can form in a number of different ways. In many cases, physical and chemical properties of diamonds unambiguously classify them as formed below cratons (xenocrystal cratonic), formed in a subducting slab followed by rapid exhumation (orogenic), or formed by crystallization directly from a host volcanic rock (phenocrystal).

Cratonic diamonds are the most common among macrodiamonds (crystals larger than 0.5 mm), and are found in kimberlites and lamproites on all continents. These diamonds characteristically display varying degrees of resorption of octahedral, cubic, and cubo-octahedral single crystals and aggregates (Robinson 1989; McCallum et al. 1994; Harris 1992). More than 99% of the diamonds have N contents below 3,500 ppm (average ~200 ppm), and in most diamonds that contain more than 20 ppm N (type I diamonds), N is present as pairs or tetrahedra (type IaA–IaB; Cartigny et al. 2004).

Orogenic diamonds are found in various metamorphic rocks from ultrahigh-pressure (UHP) terranes (e.g.

Sobolev and Shatsky 1990; Chopin 2003) of invariably continental parentage (Ogasawara 2005) or in subduction-related volcanics (Barron et al. 1996; Capdevila et al. 1999; Griffin et al. 2000). The diamonds are brought to the surface by tectonic uplift or by magmas sampling a subducting slab. Orogenic diamonds are often characterized by small size (De Corte et al. 1999; Cartigny et al. 2001). Their dominant morphology is cubic, cubo-octahedral, and octahedral single crystals, skeletal and re-entrant crystals (De Corte et al. 1999), and polycrystalline aggregates (Ishida et al. 2003; Ogasawara 2005). Orogenic diamonds rarely exhibit surface textures indicative of dissolution, and never show resorbed faces or experience non-uniform resorption (De Corte et al. 1999). High nitrogen contents (580–4,488 ppm) and low aggregation states [type Ib–IaA as reviewed in Cartigny et al. (2004)] are also characteristic of orogenic diamond populations. Subduction diamonds in UHP terranes are commonly associated with plagioclase (Sobolev and Shatsky 1990; Schertl and Okay 1994; Stockhert et al. 2001).

Phenocrystal diamonds are commonly small (<1 mm), transparent, sharp octahedrons or cubes and fibrous cubic coats, skeletal and re-entrant crystals (R. Davies, personal communication) that show little resorption (Gurney 1989; Pattison and Levinson 1995). On average, these have higher ($\sim$900 ppm) N contents than cratonic diamonds and lower N aggregation states (pure IaA with rare Ib) (Cartigny et al. 2004).

Clear-cut correlations between the tectonic settings of diamondiferous host rocks and diamond characteristics are hampered by enigmatic suites of diamonds found in calc-alkaline lamprophyres in the Archean Wawa subprovince of the Superior Craton (southern Ontario, Canada). The lamprophyres are broadly coeval with subduction-related volcanism of the 2.7 Ga Kenoran orogeny (Lefebvre et al. 2005), yet some of the diamonds they entrained are cratonic (Stachel et al. 2004). In order to understand the origin of the Wawa diamonds, we studied a suite of 80 stones from the Engagement Zone outcrop of diamondiferous breccias (Fig. 1). The diamonds from this outcrop have not been previously characterized, and they differ from diamond suites found at other occurrences of breccias 2–4 km northwest (Stachel et al. 2004). We present a detailed study of the Wawa diamonds with respect to morphology, color, cathodoluminescence (CL), nitrogen and hydrogen contents, and their mineral inclusions. The data obtained in this study reveals many unusual and enigmatic traits of the diamond suite, which cannot be fully explained by either a cratonic or orogenic diamond formation.

Diamondiferous rocks of Wawa

The studied diamonds were extracted from a 160 kg bulk sample of polymict volcaniclastic breccia (PVB), collected from trenches E (Fig. 1) on the Band-Ore Resources property, 20 km north of Wawa, Ontario. The host diamondiferous (0.2–1 ct t^{-1}, Buckle 2002) breccia represents a new type of rock (Lefebvre et al. 2005) not known on the Superior craton until recently (Band-Ore Resources Ltd Press Release, 22.11.2000). The following description of the Wawa PVB diamondiferous rocks is a synoptic overview of detailed geologic and petrographic descriptions provided in Lefebvre et al. (2005). The breccia occurs as thick, 60–110 m beds dipping to the NE at 30° and traceable along-strike in intermittent outcrop for more than 4 km, with conformable upper and lower contacts with metavolcanic rocks (Fig. 1). The breccias are intercalated with an overturned package of mafic to felsic metavolcanics dated at 2,699–2,701 ± 1 Ma (Ayer et al. 2003), which is tectonically stacked and juxtaposed along the Mildred Lake fault (Fig. 1). Breccias occur at several stratigraphic levels and become younger to the SW in continuous cross-sections. Geological observations in drill holes suggest that the Cristal breccia bed, the source for another studied suite of Wawa diamonds (Stachel et al. 2004), is older and $\sim$200 m lower in the stratigraphic sequence than the Engagement zone breccia bed, from which diamonds studied in this work were recovered. In the recurrent package to the west of the Mildred Lake fault, the Genesis breccia bed (2,744 ± 43 Ma; Stachel et al. 2004) is older than the Mumm breccia bed to the west (2,687–2,680 ± 1 Ma, J. Ayer, personal communication). The breccias are interpreted as volcaniclastic rocks deposited as lahars.

The breccias in Wawa are spatially associated with 0.5–3 m cross-cutting lamprophyre dykes. Both diamondiferous rock types were formed from calc-alkaline lamprophyric magmas and were metamorphosed to greenshist facies. The Wawa lamprophyre dykes are younger than the breccias, as the dykes (1) have been dated at 2,715-2,674 Ma (reviewed in Lefebvre et al. 2005); (2) are in observable cross-cutting relationship to PVB and felsic metavolcanic rocks; (3) are coeval with the 2.67 Ga late orogenic intrusions of gabbro and tonalites and have ''mushy'' soft contacts with them (Lefebvre et al. 2005; Stott et al. 2002), whereas PVB predate the intrusions and could be found as megaliths in them; (4) are less deformed than PVB and do not show one of the two PVB foliations related to the 2.67 Ga Wawan phase of the Kenoran orogeny (Arias and Helmstaedt 1990). Emplacement of syn- and post-orogenic calc-alkaline lamprophyre dykes at 2.7–2.67 Ga (Stott et al. 2002) was concurrent over a large area of the Superior Craton (Wyman and Kerrich 1989; Barrie 1990; Stern and Hanson 1992), including the Abitibi Greenstone Belt (Wyman and Kerrich 1993; Ayer et al. 2002).

Tectonic history

The Wawa lamprophyric magmas are broadly contemporaneous with felsic to mafic volcanic rocks and late

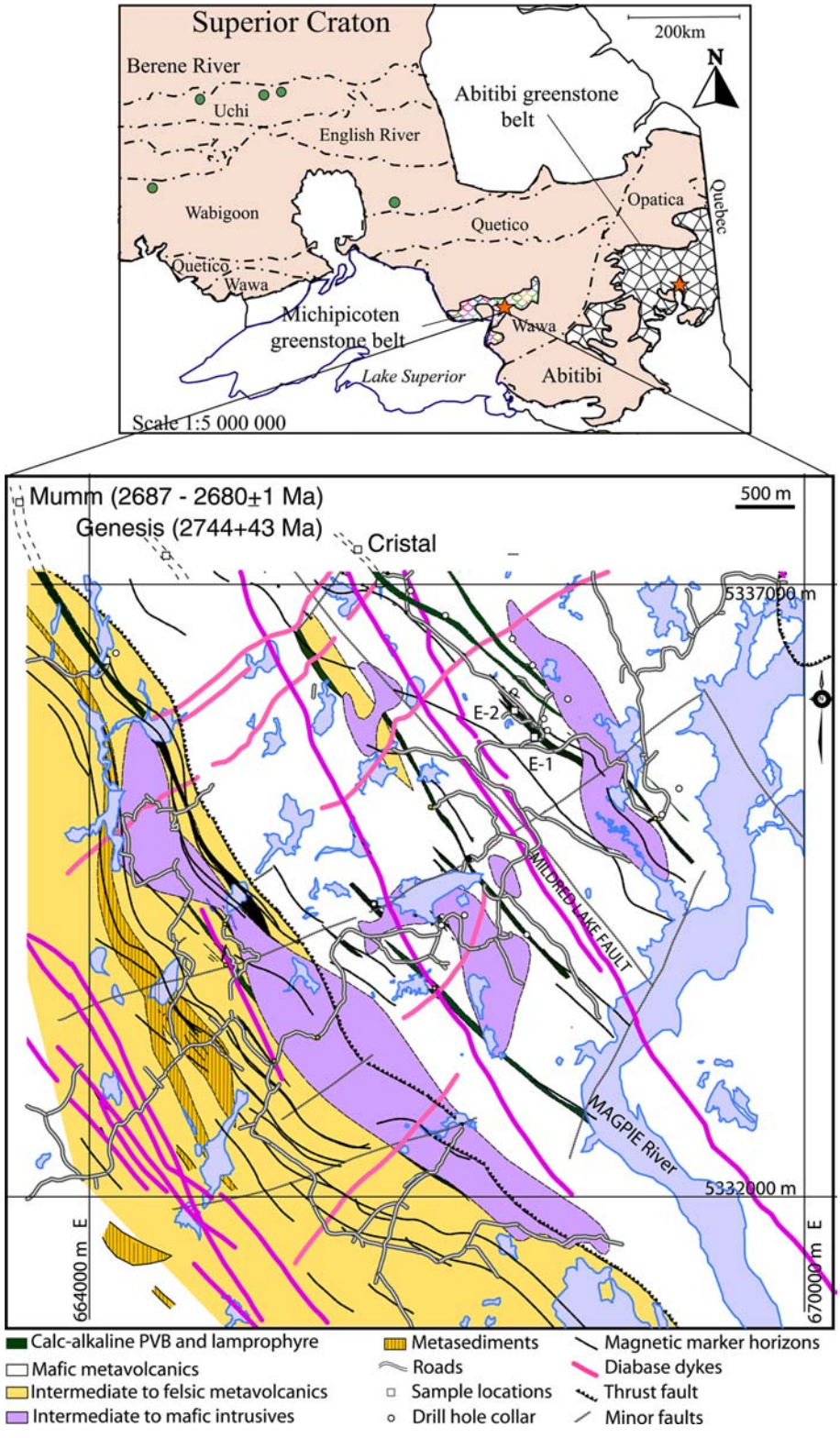

Fig. 1 Geological map of the study area in Wawa, with sampling and drill hole locations. UTM coordinates are in NAD27. *Open squares* are locations of bulk samples from where the studied diamonds were extracted: E1, E2—breccia of Engagement zone (this study), Cristal and Genesis breccia beds dated by U–Pb method on zircons (Stachel et al. 2004), Mumm breccia dated by U–Pb method (Ayer, unpublished data). The *inset* illustrates a location of the Michipicoten greenstone belt within the Wawa subprovince in the Superior craton. *Dashed lines* divide subprovinces of the Superior craton (Card and Ciesielski 1986). A *star* shows location of the shoshonitic diamondiferous lamprophyres (Wyman and Kerrich 1993; Williams 2002) within the Abitibi subprovince and *dots* show locations of calc-alkaline lamprophyres within the Uchi and Wabigoon subprovinces (Wyman and Kerrich 1989)

orogenic intrusives of magmatic cycle 3 of the Michipicoten greenstone belt (MGB), coeval with the Kenoran orogeny (Stott 1997). All three MGB volcanic cycles, dated at 2.89, 2.75, and 2.70 Ga (Turek et al. 1992), are bimodal basalt–rhyolite suites; the 2.89 Ga volcanic units also contain komatiites (Sage et al. 1996a, b). The third cycle of volcanism is represented by massive and pillowed, intermediate to mafic, tholeiitic lava flows, conformably overlain by intermediate to felsic tuff, breccia and clastic sedimentary rocks (Williams et al. 1991; Sage 1994). Intrusive rocks generated by this cycle of magmatism include gabbro to quartz–diorite sills and

dykes (Sage 1994) and syenites (Stott et al. 2002). MGB was strongly deformed by the Wawan phase of the Kenoran orogeny (ca. 2.67 Ga; Stott 1997) with four major deformational events (Arias and Helmstaedt 1990); diamondiferous PVBs are deformed by D_2 and D_4 events (Lefebvre et al. 2005).

The Superior province formed by repeated accretion of terranes as a result of subduction in a compressional margin (Hoffman 1990; Williams et al. 1991). This model is supported by seismic, structural, and geological data (Calvert et al. 1995; Calvert and Ludden 1999; Thurston 2002). While the general model of subduction and accretion has been widely accepted for the Superior craton, the tectonic origin of its individual terranes may vary.

The MGB is interpreted as an allochthonous terrane, tectonically transported to its present position, detached from its original mantle "root" (Wyman and Kerrich 2002). This allochthonous terrane can be an assemblage of island and continental arcs (Sylvester et al. 1987; Sage 1994 and references therein), or intraoceanic arcs, oceanic plateaus and trench turbidites tectonically imbricated in the north-dipping subduction zone (Sage 1994 and references therein; Polat and Kerrich 2001; Wyman and Kerrich 2002). The ~2.7 Ga voluminous volcanics of the MGB have geochemical characteristics of island arc magmas (Polat and Kerrich 2001; Wyman and Kerrich 1989, 1993) and the ~2,690 Ma Wawa lamprophyres also show strong negative Nb–Ta, Ti, and Zr–Hf anomalies (Williams 2002).

Some geological and geochronological evidence, however, is not consistent with the MGB as an allochthonous exotic terrane (Thurston 2002). The competing model advocates an autochthonous origin for the MGB, with greenstones being accumulated in place, erupting through and being deposited upon older units (Thurston 2002; Ayer et al. 2002). This model suggests that the Superior Province experienced orderly, autochthonous progression from platforms to rifting of continental fragments, all followed by late assembly during the Kenoran orogeny. This interpretation of early cycles of Michipicoten volcanics as flood basalt provinces and intra-cratonic magmatism is supported by geochemical evidence, which records crustal geochemical signatures and significant contributions from continental passive margin sources (Sage et al. 1996a, b). The cycle 3 magmatism may also have a flood basalt origin (Sage et al. 1996a, b), or may be more closely related to subduction as it is syn-orogenic (Sage 1994). The autochthonous model implies that MGB magmatism was rooted in the underlying lithospheric mantle.

Analytical methods

Morphology, body color, fluorescence, CL, nitrogen content and aggregation state, and mineral inclusions are documented for 80 diamonds ranging in weight from 0.127 to 9.343 mg (0.0006–0.047 carat) [Electronic Supplementary Material (ESM), Table 1]. Twelve thousand microdiamonds (< 0.5 mm) from the Engagement zone bulk sample have not been studied.

The CL characteristics of 63 rough diamonds from Wawa were examined using a Cambridge Instruments Cathode Luminescence (CITL 8200 mK4) system attached to an optical microscope with a 2.5× lens. The accelerating voltage used was 15 kV with an electron beam current of 300 μA and the chamber pressure was maintained using a Varian DS 102 pump. Diamonds were mounted in CL-inactive carbon putty and placed on a recessed steel tray specially designed to fit the chamber. The CL spectral characteristics of 20 selected diamonds were investigated using an Electron Optics Service (EOS) CL spectrometer attached to a Philips XL 30 scanning electron microscope. The spectrometer was a high sensitivity 2048 charge coupled device (CCD) with selected grating optimized for 360–1,000 nm spectral coverage. The acceleration voltage used was 20 kV with an electron beam current of 100 μA. Because CL emission depends on the density of the electron beam and temperature (Clark et al. 1992), all CL spectra were acquired at similar temperatures (18°C) and the analytical regime using blue CL diamonds from other locations worldwide as internal standards. The CL spectra were processed using software provided by Ocean Optics Inc and PeakFit™. Input data were first smoothed using Gaussian convolution in order to remove the noise and then deconvoluted using a Gaussian algorithm to peaks with fixed position (common CL diamond peaks such as those at 435 and 503.2 nm; Zaitsev 2001) and other peaks with variable positions. The process was then iterated until the coefficient of determination (r^2), calculated with the method of least squares, reached a value of ~0.999. The standard error in the X position of the peaks (0.2–2 nm) was calculated for 95% confidence limits.

Nitrogen content and aggregation states for 41 diamonds were determined from Fourier Transform Infrared (FTIR) spectra obtained using a Nicolet 710 FTIR spectrometer with a Nic-Plan IR microscope attachment and liquid nitrogen reservoir. Absorption spectra were measured in transmission mode in the range of 4,000–650 cm^{-1} at a resolution of 8 cm^{-1} by averaging the signals of 256 scans. The rough stones were mounted using the method of Mendelssohn and Milledge (1995) and spectra were recorded at the point of maximum light transmission through the sample. The spectra were corrected for varying diamond thickness by reference to the spectrum of type II diamond with a known thickness and using the thickness correction factor of 11.94 absorption unit cm^{-1} (Mendelssohn and Milledge 1995). One absorption unit corresponds to the absorption value at 1,995 cm^{-1}. After baselining, spectra were manipulated using Omnic version 6.0a software and were de-convoluted into several components (C, A, B, and platelet B′) using least square techniques. C-centers are single substitutional nitrogens with characteristic absorption peaks at 1,130 and 1,344 cm^{-1}; they

are absent in the Wawa stones. A-centers are pairs of N atoms, B-centers are nitrogen tetrahedra around a vacancy, and the platelet B′ component is a peak at 1,359–1,374 cm^{-1} caused by stretching of C–C bonds in planar defects on {100} planes, so called platelets (Clark et al. 1992). Based on the concentration of nitrogen and its aggregation state, diamonds are divided into type I (stones with >20 ppm N) or II (stones with no measurable N). Type I diamonds are further subdivided into type Ib (stones with unaggregated N), type IaA (stones containing mainly A-centers), type IaB (stones containing mainly B-centers), as well as into transitional groups (diamonds with A, B or A and B-centers) (Evans 1992). Nitrogen concentrations (in atomic ppm and in percentages of the total nitrogen content) were calculated on the basis of the 1,282 cm^{-1} absorption peak using the Boyd et al. (1994, 1995) formulas for quantification of A- and B-centers, respectively. Detection limits and errors, according to Stachel and Harris (1997) and Stachel et al. (2002), are strongly dependent on the quality of the crystal face, but typically range between 10 and 20 ppm or 10–20% of the concentration, respectively. Additional uncertainty is introduced by the heterogeneity of nitrogen content within the different growth layers of diamond (Taylor et al. 1990). Hydrogen concentrations (in relative absorption units) were calculated by measuring the difference between the base and peak height at 3,107 cm^{-1}. The error for hydrogen values reported is estimated at 2.6 rel.% and the minimum detection limit is estimated at 0.03 cm^{-1} absorption units for a diamond of 1 cm thickness. Infrared absorption spectra were difficult to obtain for many of the opaque and translucent diamonds, and those with highly irregular surfaces, especially fine-grained aggregates.

Sixty-three inclusions were extracted from 14 host diamonds by mechanical crushing in an enclosed steel cracker. Exposed inclusions on a diamond chip surface were examined in a back scattered electron (BSE) mode on the SEM. Quantitative electron probe microanalysis (EPMA) was performed on a fully automated CAMECA SX-50 microprobe, operating in the wavelength-dispersion mode with the following operating conditions: excitation voltage 15 kV; beam current 20 nA; peak count time 10 s; beam diameter 3 μm. A variety of well-characterized minerals and synthetic phases were used as standards. The minimum detection limits for most oxides are less than 0.06 wt%. Exceptions to this include Cr_2O_3 (0.16 wt%), FeO (0.08 wt%), MnO (0.08 wt%), and NiO (0.10 wt%). Relative errors, at the 2σ confidence level, are estimated to be <2% at the >10 wt% level, 5–10% at the ~1 wt% level, 10–25% at the 0.2–1 wt% level, and 25–50% at the <0.1 wt% level.

Morphology and colors

The Wawa diamonds are highly variable in their primary growth forms (Fig. 2). The majority of diamonds are either octahedral aggregates (Fig. 2e) (44% of the population) or single octahedral crystals (Fig. 2d) (26%). The sizes of crystals in the aggregates are typically >0.5 mm, to (less commonly) 0.1–0.5 mm. Single cubic and cubic–octahedral crystals and their aggregates (Figs. 2a–c), as well as macles are also observed (Fig. 2f); 48% of the Wawa diamond population in this study are single crystals. Only 28 diamonds could be evaluated for crystal regularity because the majority of samples are broken crystals and fine aggregates. The majority of the Wawa diamonds are distorted to some degree, and only 11% are near-equidimensional.

The Wawa diamonds in this study are colorless (50%), heterogeneous (24%), yellow (11%), black (3%), brown (10%), and gray (3%). All cuboids including the cubic aggregates are yellow in color, but not necessarily translucent. The majority of octahedral single crystals

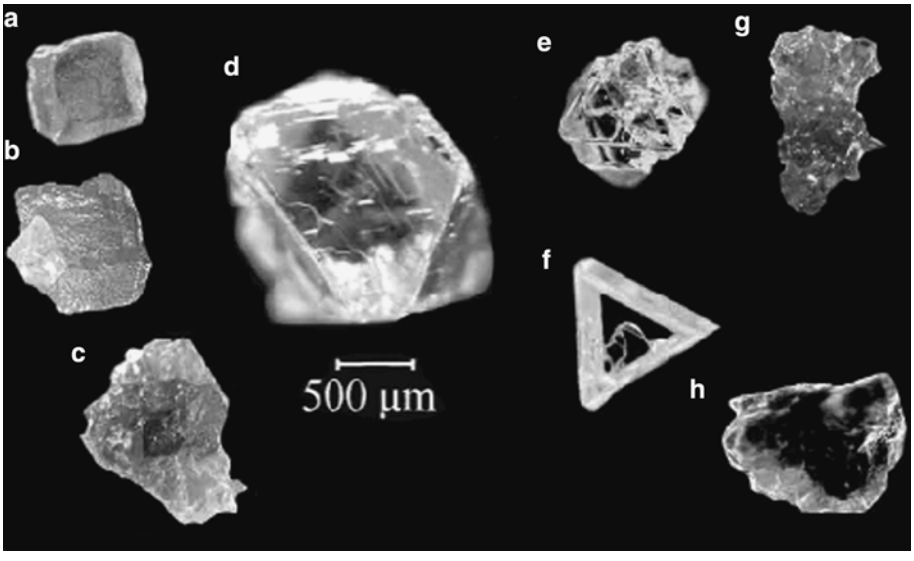

Fig. 2 Varying crystal habiti of the Wawa diamond population. **a** cube, **b** coarse aggregate of cubic crystals, **c** cubo-octahedral aggregate, **d** octahedron, **e** octahedral coarse aggregate, **f** macle, **g** octahedral fine aggregate, **h** octahedral aggregate

and coarse aggregates, as well as all macles, are colorless. The heterogeneity in color is present only in aggregates (ESM Table 1). The Wawa diamond population consists of 48% transparent crystals, 25% translucent crystals, 14% opaque crystals, and 14% combination of opaque and translucent crystals. The transparent crystals are mostly colorless and also comprise a few yellow octahedral single crystal and coarse aggregates, as well as macles. The translucent crystals comprise all possible primary crystal forms and colors. The opaque crystals are mostly fine-grained aggregates which have some black body coloring.

The diamonds in general have experienced low degrees of resorption (Figs. 2d–f, 3b). Over half of the diamonds fall into resorption classes 4–6 of McCallum et al. (1994), with 22% in class 4, 38% in class 5, and 8% in class 6. Diamonds which have experienced extensive resorption (class 1–3) comprise only 21% of the population. Some crystals (14%) exhibit non-uniform resorption, whereby one part of the crystal is more strongly resorbed than another (ESM Table 1). Resorption specific to octahedral crystals and octahedral faces on cubic–octahedral crystals is marked by the presence of shield-shaped laminae, trigonal pits, hexagonal pits, hexagonal pits containing etch pits, and serrate laminae (terminology by Robinson 1989). Tetragonal pits are developed on cubic crystals and the cubic face of cubic–octahedral crystals. Other surface features specific to highly resorbed tetrahexahedroid crystals are terraces and elongate hillocks which are seen on only 4 and 1% of the Wawa diamonds, respectively. Late stage etching features present on some diamonds of all resorption classes are ruts, shallow depressions, frosting, and corrosion sculpture. The diamonds carry no evidence of deformation such as lamination lines.

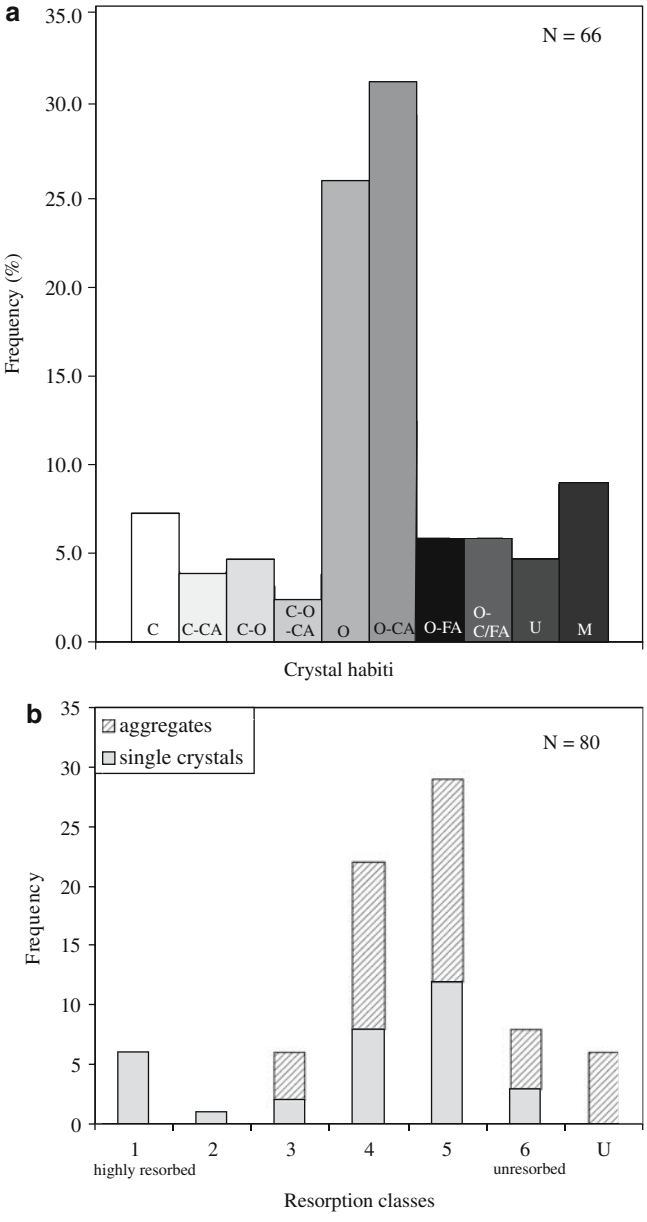

Fig. 3 **a** Histogram showing frequency of occurrence of different crystal habiti in the Wawa diamond population. *Symbols*: *C* cubic, *C-CA* cubic-coarse aggregate, *C-O* cubo-octahedral, *C-O-CA* cubo-octahedral coarse aggregate, *O-CA* octahedral coarse aggregate, *O-FA* octahedral fine aggregate, *O-C/FA* octahedral heterogeneous aggregate, *U* unknown, *M* macle. **b** Histogram showing the frequency of occurrence of resorption classes in Wawa diamonds and the relative abundances of single crystals and aggregates. Resorption classes follow the classification scheme of McCallum et al. (1994)

Cathodoluminescence

Diamonds are grouped into six categories based on observed optical CL colors (ESM Fig. 1). The relative abundances of CL colors, based on the analysis of 69 diamonds, are as follows: orange-red (46%), yellow (28%), orange-green (10%), green (6%), and other non-uniform colors (10%). Interestingly, none of the Wawa diamonds exhibited common blue CL. The description of CL spectra (Fig. 4) below is based on the PeakFit deconvolution results. The procedure finds unequivocal positions of only sharp peaks and assigns a non-unique combination of peaks to wider maxima. Therefore, we give precise positions of the peaks only if they are stable irrespective of the parameters of the deconvolution.

In diamonds with the red-orange CL color, the SEM-CL spectral analysis reveals a sharp line at 575.5 nm, typically associated with several broader peaks in the red region of the spectrum between 586 and 664 nm. Broad peaks of lower intensity are also observed in the green region (around 520 nm) and in the blue region (around 440 nm) (Fig. 4). The relative intensities of the peaks show considerable variations in different samples and also in different spots of the same sample.

In diamonds with yellow and green-yellow CL, the main peak occurs in the green region of the visible spectrum around 520 nm. The sharp line at 575.5 nm is also present, although it was not observed in all samples and all the analyzed spots (Fig. 4). The asymmetric

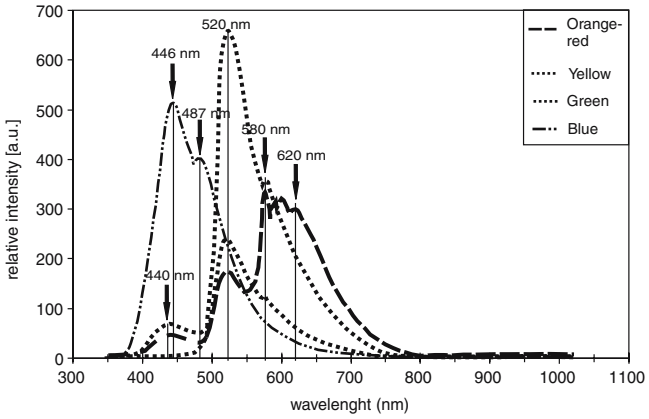

Fig. 4 A plot of CL emittance intensity (in arbitrary units) versus emitted wavelengths (in nm) for Wawa diamonds representative of different CL colors. A CL spectrum of a diamond from Rio Soriso (Brazil) with typical blue cathodoluminescence is shown for comparison. Spectra were integrated for 5 s from the beginning of the electron beam irradiation

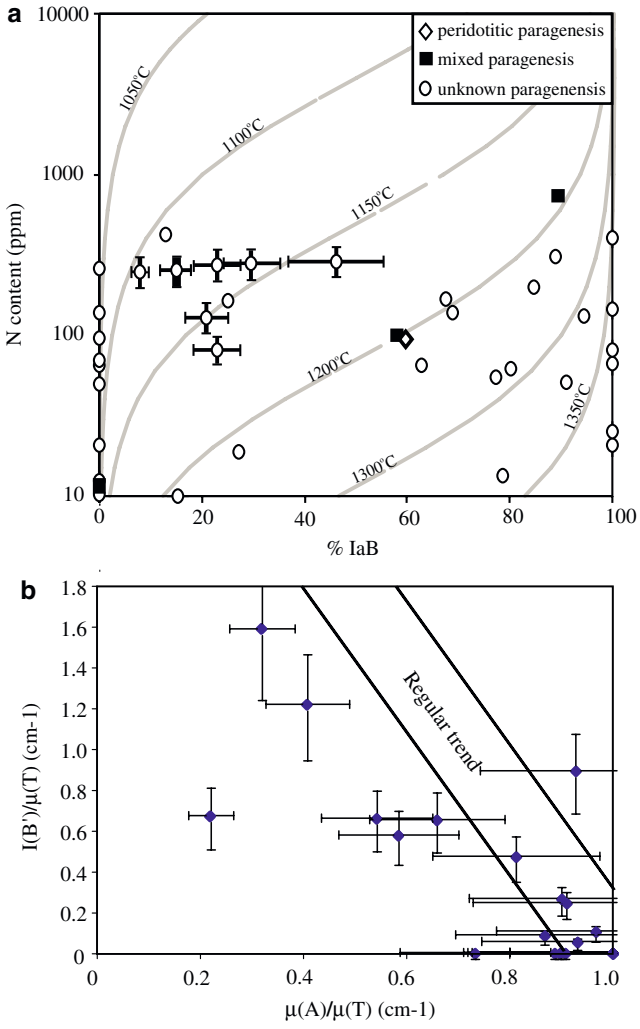

Fig. 5 **a** A plot of nitrogen concentration (ppm) versus content of B-centers (%IaB). Isotherms were calculated using the method of Taylor et al. (1990) for the 1.8 Ga mantle residence time. The estimated temperatures are valid only for regular diamonds that are marked on the plot with *error bars*. The *bars* correspond to 20% error from the detection limits and deconvolution method (Stachel et al. 2002). Where possible, diamond parageneses are inferred from inclusion studies. **b** A plot of platelet peak intensity [I(B′)—absorption value of B′ peak after subtraction of the 2-phonon tail] divided by total absorption (μT) versus strength of A-center absorption (μA) divided by total absorption (μT). The *error bars* correspond to the 20% uncertainty propagated through the functions plotted on X and Y axes. The regular trend is from Woods (1986).

shape of the main 520 nm band deconvolutes to several smaller peaks between 543 and 610 nm.

In diamonds with green CL, the main peak also occurs at 520 nm. In samples with good spectral resolution, a sharp line at 575.5 nm is also observed. A broad peak of variable intensity at 440 nm is present in most samples (Fig. 4). The asymmetry of the 520 peak suggests the presence of additional peaks at 548–616 nm.

In summary, CL emittance of all Wawa diamonds consists of a broad band at ~520 nm, a sharp peak at 575.5 nm, and several lines at 550–670 nm. In contrast, diamonds with common blue CL feature prominent wide peaks at ~430–450 and 480–490 nm (Lindblom et al. 2003) (Fig. 4).

Impurities in Wawa diamonds

FTIR spectroscopy indicates that the studied diamonds contain nitrogen and hydrogen. The majority of Wawa diamonds have low nitrogen contents, below 300 ppm (Fig. 5a). The nitrogen contents range between 0 and 740 atomic ppm (ESM Table 1), with a mean nitrogen content of 111 ppm, a median of 66 ppm, and a mode below detection limit.

Nitrogen initially enters the diamond lattice as single substitutional atoms, aggregating at high temperatures over time to pairs (A-centers), and then to four nitrogen atoms (B-centers). The progressive aggregation of A- to B-centers can also result in simultaneous formation of platelets readily identified by their B′ peak (Woods 1986). In such "regular" diamonds (Woods 1986), the intensity of the B′ peak is inversely proportional to the intensity of a peak characteristic of the A-center (Fig. 5b). If diamonds are stored in the mantle for a greater period of time, or at increased temperatures, or if they experience plastic deformation, aggregation will continue to advance and platelets, along with A-centers, will concurrently degrade and disappear entirely. Such diamonds are known as "irregular" (Woods 1986; Clark et al. 1992). An apparent "irregular" character of many diamonds worldwide may be an artifact of bulk FTIR measurements on stones that are zoned with respect to N content and aggregation (R. Davies, personal communication).

The Wawa diamonds show variable degrees of nitrogen aggregation. The majority of Wawa diamonds are

Table 1 Characteristics of the Wawa diamonds with mineral inclusions

Sample number	Morphology	Resorption class[a]	Color	Trans parency	CL color	N (ppm)	%B	H peak at 1,307 nm (relative absorption units)	IR spectrum classification	Inclusions		Paragenesis
										Primary	Secondary	
GQE4-2	O	5	CL	TP	Or	95	59	–	Type IaAB?	2 Ol		Peridotitic
GQE4-7	O-CA	5	CL	TP	Y	< mdl	–	–	Type II	1 Ol, 2 Cpx	1 Ap, 1 Bt, 1Chl	Mixed
GQE4-8	O-CA	4	CL	TP	Y	< mdl	–	–	–	1 Ol, 1 Cpx,	1 Al-Sil.	Mixed
GQE4-11	C	5	Y	TL	Or	251	14	–	Type IaAB		1 Al-Sil.	
GQE4-19	O	5	CL	TL	Y	100	100	–	Type IaB?		4 Chl	
GQE5-1	O-CA	5	CL	TP	Y	NA	–	–	–	1An, 1Cpx,	1 Al-Sil.	Eclogitic
GQE7-1	O-CA	4	BR	TP	P/Y	< mdl	–	–	Type II		1Al-Sil., 2 Chl, 1 Na–Mg Sil.	
GQE8-4	O-C	U	CL/GY/BL	TL/Op	G	< mdl	–	–	Type II		1 Bt	
GQE10-2	O	5	CL	TP	G/Or	145	100	0.10	Type IaB?		3 Bt, 1 Na–Mg Sil.	
GQE10-3	O-CA	2	GY	TL	Y	101	58	–	Type IaAB?	1 Ol, 2 Opx, 1 Cpx,	2 Chl	Mixed
GQE11-2	O	4	C	TL	Or/Y	NA	–	–	–		1 Al-Sil.	
GQE13-2	O	3	BR	TL	Or	< mdl	–	–	Type II	1 Ni–Fe Sulph., 1 An		Peridotitc or eclogitic
GQE14-1	C-O/A	4	Y/GY	TL/Op	Or	49	0	–	Type IaA?		2 Chl	
GQE14-2	O	U	GY/CL	TL/Op	Or	13	0	–	Type II		1 Chl	
GQE14-3	O-CA	6	CL	TP	Or	740	90	0.21	Type IaAB	4 Ol, 2 Cpx, 2 Ni–Fe Sulph.	1 K–Ni–Fe sulph., 1 Bt, 5 Chl	Mixed
GQE14-4	C-CA	4	Y	TL	Or	96	0	–	Type IaA		3 Chl, 1 Ap	
GQE15-1	O	5	CL	TP	Or	< mdl	–	–	Type II	4 Ol, 1 Opx, 1 Ab	1 Fe-Al Sil., 1 K Fsp	Peridotitic
GQE16-1	O	5	CL	TP	Or/G	< mdl	–	–	Type II			
KD4243-1	M	5	CL	TP	NA	NA	–	–	–	3 Ol, 1An		Peridotitic
KD4220-2	O	1	CL	TP	NA	NA	–	–	–	2 Ol		Peridotitic

Abbreviations: *O* octahedral, *C* cubic, *A* aggregate, *M* macle, *U* unknown, *CL* colorless, *BL* black, *BR* brown, *Y* yellow, *GY* gray, *TP* transparent, *TL* translucent, *Op* opaque, *G* green, *Or* orange, *P* pink, *B* blue, *< mdl* below minimum detection limit, *NA* not analyzed, *Ol* olivine, *Opx* orthopyroxene, *Cpx* clinopyroxene, *Bt* biotite, *Chl* chlorite, *Ab* albite, *An* anorthite, *Fsp* feldspar, *Ap* apatite, *Sil.* silicate, *Sulph.* sulphide[a]Resorption classes are determined according to the classification scheme of McCallum et al. (1994)

type IaAB (49%) and type IIa (34%); the remainder are type IaA (17%) (Fig. 5a). Nitrogen aggregation states show a possible bimodal distribution (Fig. 5a): the first mode, where the majority of the samples occur, has < 30% aggregation in the B-form (mostly type II and type IaA diamonds); the second mode has a high aggregation state, with > 60% B (group median 79% B). The higher abundance of B-centers does not correlate with a higher nitrogen content (ESM Table 1), which is typical for most diamonds around the world (Stachel and Harris 1997), suggesting different temperature–time histories. Of the type IaAB diamonds, 67% contain platelets; 33% diamonds with low aggregation states (< 25% B-defect) do not have platelets developed. Sixty-five percent of the diamonds are irregular and show much lower platelet peak intensities than would be expected from their content of A-centers (Fig. 5a). Wawa type IaA diamonds do not contain either platelet peaks or B-defects, consistent with the observations of Woods (1986).

Conversion of N from type IaA to IaB has been quantified by Taylor et al. (1990), who show that it is largely controlled by temperature and time. The temperatures of the mantle residence, however, should only be calculated for regular diamonds with no evidence of platelet degradation (Evans 1992). The six regular diamonds from the studied suite are estimated to have remained at 1,108–1,164°C for 1.8 Ga (Fig. 5a). The assumed maximum residence time of 1.8 Ga (based on the 4.5 Ga age of the Earth and the 2.7 Ga diamond emplacement age) provides the lowest possible temperatures that could have been experienced by the diamonds. However, the temperatures are relatively insensitive to the mantle residence time as its increase by ~2 Ga results in ~150°C decrease in the estimated temperatures.

The presence of hydrogen in the studied diamonds is inferred by the presence of weak FTIR peaks detected in 60% of the samples in the 2,750–3,300 cm^{-1} range (McNamara et al. 1997) and sharp low intensity peaks at 3,107 cm^{-1} observed in ~5% of the diamonds (ESM Table 1). The 1,405 cm^{-1} H peak is not present.

Mineral inclusions

From the 14 diamonds selected for inclusion studies, 15 different phases have been analyzed, comprising 63 separate grains (Table 1). Inclusions were classified as primary or secondary based on their appearance under the SEM and on their positions within the diamonds. Inclusions of primary origin appear as competent faceted grains homogeneous in color and chemical composition (Fig. 6a–c), not associated with any cracks in the host diamonds. By contrast, inclusions classified as secondary occur as amorphous inhomogeneous grains, often bound to fractures in the diamond (Fig. 6d, Table 2). Listed in order of decreasing abundance, the primary inclusions recovered include olivine, clinopyroxene, orthopyroxene, Fe–Ni sulphide, and plagioclase (Table 2).

Olivine is the most abundant mineral inclusion in the diamonds. Eighteen olivine grains (5–80 μm; Fig. 6a) are identified in eight diamonds. Two different populations of olivine are observed. The first population has Mg# = molar Mg/(Mg + Fe) between 0.92 and 0.93, typical of subcratonic low-T peridotite and abyssal and ophiolitic peridotites (Boyd 1989). The second population is higher in Fe and shows Mg numbers of ~0.89, common to the most mantle peridotites worldwide, as well as mafic igneous rocks and high-T cratonic peridotites (Pearson et al. 2002). The NiO content is the same in both types of olivine and equal to 0.31–0.36 wt%. High-Mg olivine is found together with orthopyroxene, clinopyroxene, albite, anorthitic plagioclase, and Fe–Ni sulphide, whereas Fe-rich olivine is only found in one diamond KD4243-1 in association with an anorthitic plagioclase (Table 1).

Seven clinopyroxene grains (5–15 μm) are identified in six diamonds in association with high-Mg olivine, orthopyroxene, plagioclase, and Fe–Ni sulphide (Table 1). EDS spectra of Wawa clinopyroxenes suggest that all grains have similar Cr-free, Fe-rich compositions. Due to the small size of the clinopyroxene inclusion, only one grain yielded a reliable quantitative chemical analysis (Table 2). This grain shows low Mg# (~0.65) and very low Cr_2O_3 (~0.09 wt%) content and is classified as omphacite with 14 mol% jadeite. The Wawa omphacite is similar to K_2O-rich eclogitic clinopyroxenes in diamonds (as compared to the worldwide database of Stachel et al. 2000). Concentrations of K_2O contents above 0.5 wt% are found in one-third of all worldwide eclogitic clinopyroxene inclusions (Fig. 6 of Stachel et al. 2000) which may or may not occur together with the transition zone majorite.

Four plagioclase grains (8–15 μm), pure albite and anorthite (An)-rich plagioclase, are recovered from the Wawa diamonds (Table 2). Albite is found with olivine and orthopyroxene, whereas An-rich plagioclase is found with clinopyroxene. Plagioclase is an extremely rare syngenetic inclusion in diamond. Pure albite was found in a Roberts Victor diamond of unknown affinity; more calcic plagioclases ($Ab_{18.5}$ and $Ab_{62.4}$) are documented in eclogitic and peridotitic diamonds together with eclogitic garnet and olivine (Fo_{91}), respectively (Viljoen et al. 1999). While An-rich plagioclase can be found in shallow peridotites (Pearson et al. 2002), it cannot be in equilibrium with diamond (Fig. 7). Similarly, An-rich plagioclase can occur in eclogites as a relic from amphibolite or granulite facies metamorphism (Pearson et al. 2002), and plagioclase becomes more albitic after partial eclogitization (e.g. Miller and Thoni 1997), but completely equilibrated diamondiferous eclogites should not contain plagioclase.

Three orthopyroxene grains (5–60 μm; Fig. 6b) are found in two diamonds. The orthopyroxenes show high Mg# (0.93) and low (~0.3 wt%) Al_2O_3 contents. The orthopyroxenes clearly belong to the equilibrated peridotitic paragenesis as its Mg number is slightly higher than the Mg number of the coexisting olivine (Pearson

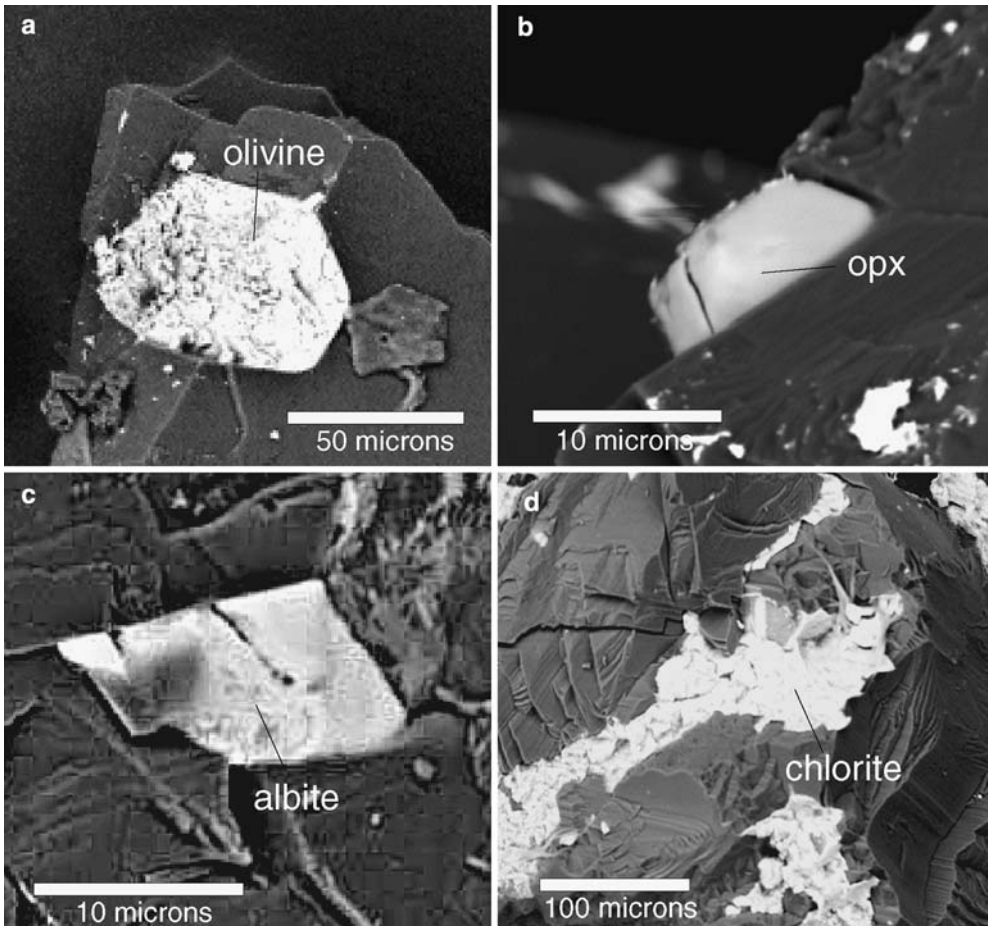

Fig. 6 Microphotographs of mineral inclusions in Wawa diamonds: **a** olivine (sample KD4243-1), **b** orthopyroxene (GQE10-3), **c** albite (GQE15-1), **d** secondary chlorite developed along a diamond crack (GQE14-1)

et al. 2002). Judging by Al_2O_3 below 2 wt%, orthopyroxenes were equilibrated in the garnet facies of mantle peridotites (Smith 1999).

Two Ni–Fe sulphide inclusions (< 10 μm) are identified in two diamonds. They are found in association with high-Mg olivine, orthopyroxene, clinopyroxene, and plagioclase (Table 1). Sulphide grains are homogeneous in composition and are classified as Fe-rich pentlandite. Its high Ni content (25 wt% Ni; Table 2), however, cannot be taken as a proof of its peridotitic origin. There is no clear dichotomy in compositions of sulphides in eclogitic and peridotitic diamonds on the Kaapvaal craton (Pearson et al. 2002), and unpublished data shows that high-Ni sulphides such as pentlandites (15–34% Ni) and millerite (49–72% Ni) are very common in the Slave craton eclogite, as evidenced by Jericho and Lac de Gras (S. Aulbach, personal communication) kimberlite xenoliths.

Discussion

Cathodoluminescence

The CL colors displayed by the majority of Wawa diamonds (orange, yellow, and green) are relatively rare. Most natural diamonds cathodoluminesce blue (Bulanova 1995); red CL colors are only noted for irradiated natural diamonds (Milledge et al. 1999; Zaitsev 2001) and for N-doped non-annealed diamonds grown by the carbon vapor deposition (CVD) process (Martineau et al. 2004). Yellow CL colors are detected in carbonado, a dark-colored cryptocrystalline porous diamond (Magee and Taylor 1999), and in low-N diamonds (R. Davies, personal communication). Some of the orogenic microdiamonds in the Kokchetav massif cathodoluminesce green (Yoshioka and Odasawara 2005). CL spectroscopy allows a comparison between the studied Wawa diamonds and diamonds with visibly similar CL.

Most blue CL natural diamonds show a broad luminescence band at 400–490 nm (Lindblom et al. 2003) or several peaks in these wavelengths (Fig. 4). The most common of these CL features are a peak at ~415 nm linked to three nitrogen atoms with a vacancy (N3 center) in diamonds with a highly aggregated N, and an A-band (415–443 nm) (ESM Table 2). In contrast, CL colors of Wawa diamonds are controlled by emission at longer wavelengths above 500 nm, although the A-band is present as a subordinate peak (Fig. 4).

The CL of Wawa diamonds cannot be fully explained from their low-N character. The A-band (ESM Table 2), the main CL feature of low-N (type IIa) diamonds, is observable on studied diamonds with N content below 70 ppm (26 out of 46 stones). However, even in these

diamonds, the predominant CL peaks are above 500 nm.

The CL characteristics of the Wawa diamonds cannot be explained by processes that created CVD diamonds with red CL. Some CVD diamond spectra (for N-doped annealed stones) do not show any CL peaks at wavelengths longer than 575 nm (Martineau et al. 2004), whereas most red CL Wawa diamonds feature numerous peaks between 578 and 622 nm in their spectra (ESM Table 2). In other CVD diamonds, CL emittance at wavelengths >575 nm (596/597 nm doublet) anneals at mantle temperatures and is caused by single substitutional N (Martineau et al. 2004). Such N is absent in Wawa diamonds.

The CL spectra of some Wawa diamonds resemble those of Kokchetav microdiamonds with only one broad emission band at 514–537 nm. This "green" band (ESM Table 2) occurring at around 520 nm in all Wawa diamonds is the main peak for the studied stones that cathodoluminesce yellow and green (Fig. 4). The broad "green" band is detected in some samples of carbonado where it is ascribed to the sharp 525 nm doublet observable in the photoluminescence spectrum (Magee and Taylor 1999).

Overall, the CL spectra of Wawa diamonds resemble most the CL spectra of carbonado with yellow and green CL (Magee and Taylor 1999); peaks at 520 and 575 nm are prominent in Wawa and carbonado samples. However, CL emission of Wawa stones and carbonado differ at wavelengths above 630 nm. In Wawa diamonds, the CL emission at these wavelengths is practically absent, whilst carbonado shows a plateau or a broad peak (Magee and Taylor 1999). The 575 nm peak in carbonado results from irradiation as (1) the peak was reproduced by irradiation in polycrystalline cintered diamonds (Zaitsev 2001), the analogue to natural carbonado; and (2) red (Milledge et al. 1999), yellow, and orange (Magee and Taylor 1999) CL colors in carbonados are mapped as concentric haloes around radioactively damaged spots. The 575 nm peak, however, cannot be ascribed to irradiation in the Wawa diamonds as they show no evidence of radioactive damage such as coloration haloes, visible either optically (Vance and Milledge 1972) or in CL (Milledge et al. 1999). The red CL emission in Wawa diamonds is more realistically interpreted as a result of defects on interstitial O or C, a vacancy or B′ platelets (ESM Table 2). Whatever the process was that led to atypically defective lattices of the diamonds, it must be significantly different from common diamond-forming processes.

Diamond paragenesis

The Wawa diamonds host primary inclusions of peridotitic (P) and eclogitic (E) paragenesis. Olivine and orthopyroxene are peridotitic in origin, clinopyroxene is eclogitic, whereas plagioclases and sulphide are compatible with either of these assemblages. Most of the mineral inclusions are unequilibrated both with each other and with the host diamond. Inclusions of peridotic and eclogitic affinities are found together in four diamonds (40% of the diamonds where inclusions are studied), whereas in most diamond inclusion studies, mixed paragenesis is "the exception rather than the rule" (Gurney 1989). The rest of the diamonds contain peridotitic (4 diamonds, 40%), eclogitic (1, 10%), or an indeterminate paragenesis (1, 10%) which may be either peridotitic or eclogitic. Moreover, many P- or E-type Wawa diamonds contain a low-pressure phase (plagioclase), incompatible with the diamond stability field. Thus, the majority (80%) of the diamonds shows either gross compositional disequilibrium, combining peridotitic and eclogitic minerals or thermodynamic disequilibrium, combining shallow and deep minerals. The unequilibrated assemblages of inclusions defy a simple explanation. Two petrogenetic models which we propose for these diamonds are (1) complex growth history of diamonds, or (2) pervasive alteration of primary inclusions through now annealed fractures in diamonds.

A subduction setting is crucial for the first model. The diamonds must have grown in the mantle and in crustal portions of the slab, as evidenced by their occurrence in the peridotitic and eclogitic assemblages. The *P–T* stability field of eclogite in the slab matches the depths and temperatures of the diamond stability there (>110 km, Fig. 7). The plagioclase found in the Wawa diamonds may be a relic, inherited from the prior existence of the oceanic lithosphere at shallower depths where it is stable as plagioclase peridotite or mafic granulite. A repeated observation in HP/UHP terranes that have been subducted and then exhumated is that significant rock volumes may escape mineral equilibration at the prevailing *P–T* conditions, despite *T* as high as 650–750°C for UHP rocks (Chopin 2003). High rates of subduction in the Archean (Staudigel and King 1992) and equally rapid emplacement of UHP terranes (Rubatto and Hermann 2001) make these blocks ideal for preservation of metastable assemblages. Moreover, plagioclase is known to coexist with diamond in UHP terranes (e.g. Schertl and Okay 1994; Stockhert et al. 2001). The coexistence of eclogitic and peridotitic minerals within single diamonds (as reviewed in Gurney 1989; Schulze et al. 2004) and in a single xenolith (Sobolev et al. 1997) is not unknown, although it has not been previously reported on the same scale of occurrence as we observe in the Wawa suite. The bulk compositional disequilibrium can be explained by fine-scale mixing of metamorphosed crustal and mantle material of the subducted slab during upward advection in a "cold plume". This phenomenon, inherent to convergent margins, has recently been modeled by Gerya and Yuen (2003) who demonstrate the feasibility for upwellings of material 300–400°C colder than the ambient mantle, which emanates from the top surface of the descending lithosphere and passes through the mantle wedge with ascension rates of approximately 10s of cm per year.

Table 2 Microprobe analyses of inclusions in Wawa diamonds

Mineral	Olivine	Olivine	Olivine	Orthopyroxene	Clinopyroxene	Albite		Fe–Ni sulphide
Inclusion number	77-3	80-1	9-2	40-2	52-2	54-1		46-2
Host diamond	KD4243-1	KD4220-2	GQE4-2	GQE10-3	GQE15-1	GQE14-3		
SiO_2	39.62	40.81	41.39	57.78	54.62	66.85	S	36.49
TiO_2	< mdl	< mdl	< mdl	< mdl	0.31	0.54		
Al_2O_3	0.04	< mdl	< mdl	0.34	3.38	19.27		
Cr_2O_3	0.06	0.07	0.05	0.23	0.09	< mdl		
FeO	12.13	6.78	6.53	4.22	9.74	1.05	Fe	35.46
MgO	46.42	50.17	50.30	36.21	17.78	0.05	Co	0.46
MnO	0.14	0.09	0.10	0.08	0.24	0.24	Cu	0.40
CaO	0.04	< mdl	0.41	0.41	10.63	0.03		
Na_2O	0.04	< mdl	< mdl	0.03	1.94	11.18		
NiO	0.31	0.36	0.35	0.11	0.18	0.08	Ni	25.05
K_2O	< mdl	< mdl	< mdl	< mdl	0.58	0.06		
Total	98.80	98.32	98.79	99.43	99.47	99.38		97.92
Si^{4+}	0.996	1.004	1.011	1.986	1.993	2.957		
Ti^{4+}	NA	NA	NA	NA	0.008	0.018		
Al^{3+}	0.001	< mdl	< mdl	0.014	0.145	1.005		
Cr^{3+}	0.001	0.001	0.006	0.006	0.002	NA		
Fe^{2+}	0.255	0.139	0.133	0.121	0.297	0.039		
Mg^{2+}	1.739	1.840	1.832	1.855	0.967	0.003		
Mn^{2+}	0.003	0.002	0.002	0.002	0.007	0.009		
Ca^{2+}	0.001	NA	< mdl	0.015	0.416	0.001		
Na^{+}	0.002	0.001	< mdl	0.002	0.137	0.959		
Ni^{2+}	0.006	0.007	0.007	0.003	0.005	NA		
K^{+}	NA	NA	NA	0.001	0.027	0.004		
Total	3.004	2.996	2.995	4.005	4.006	4.999		

Primary An-rich plagioclase is identified by EDS spectrometry. The diamonds also contain secondary inclusions of Fe-rich biotite and chlorite, a Na–Al–Mg–Fe silicate (smectite? glauconite?), an Al-rich silicate (Al_2SiO_5 polymorph?), Al-poor silicate (kaolinite? pyrophyllite?), K feldspar and K–Ni–Fe sulphide (djerfisherite?), Cu–Sb sulphide, K titanate (mathiasite? jeppeite?) and Sr-free apatite < *mdl* below detection limit, *NA* not analyzed

The second model suggests that compositions of the inclusions are not representative of the initial compositions of syngenetic minerals, but rather are pseudomorphs. The atypical alteration of minerals that form fresh well-faceted grains, all enclosed by an apparently non-fractured diamond, may be related to the attributes of the host Wawa volcanics. The volcanics are older than most diamondiferous primary rocks that are generally emplaced after 1.6 Ga (Heaman 2004). The volcanics have also been metamorphosed and deformed by a major orogenic event. Both of these traits increase the potential for the diamonds to be fractured and annealed, and also brings the diamonds into contact with hydrothermal and metasomatizing fluids.

Evidence for late penetration of hydrous fluids rich in K, Na, Fe, Al, and Si is found in the presence of abundant chlorite, biotite, apatite, various silicates rich in Al, Ca, and Na, K-feldspar, and K sulphides in cracks in the diamonds (Table 2). Most of these minerals can be related to host diamondiferous rocks, i.e. either be the lamprophyric phenocrysts, or a part of the greenshist assemblage. Clinopyroxene, biotite, plagioclase (Ab_{89}), and hornblende are considered to be primary phenocrysts of the Wawa host-rock magmas, whereas chlorite, actinolite, albite, and metamorphic biotite comprise the ensuing greenshist assemblage (Lefebvre et al. 2005). Djerfisherite is known to occur in lamprophyres (Rock 1991). Strontium-free apatite, phlogopite and biotite, clinopyroxene, potassic feldspar (Ort_{97}–Ab_{98}), plagioclase (An_{50}–An_6), and olivine (now completely altered), along with other minerals, have been documented as having crystallized from Archean lamprophyres of Abitibi (Wyman and Kerrich 1993) and barren Archean lamprophyre dykes of Wawa located to the northwest of our study area (Williams 2002).

Formation of Wawa diamonds

The studied suite of diamonds is atypical of most worldwide diamond suites in many aspects. First, it is hosted by Archean metamorphosed calc-alkaline lamprophyre rather than kimberlite or lamproite. Second, the diamonds show yellow-orange-red CL and contain mineral inclusions not in equilibrium with each other or their host diamond. How and where could such diamonds have formed?

The studied suite of Wawa diamonds is unlikely to have crystallized from the host lamprophyres. The following characteristics of the Wawa diamonds are incompatible with diamond phenocrysts: (1) the presence of non-uniformly resorbed and etched diamonds; (2) the low proportion of fibrous cubic diamonds; (3) the presence of distorted diamonds shapes; (4) the high nitrogen aggregation states (> 50% B-centers) indicative of long mantle residence times or high mantle residence

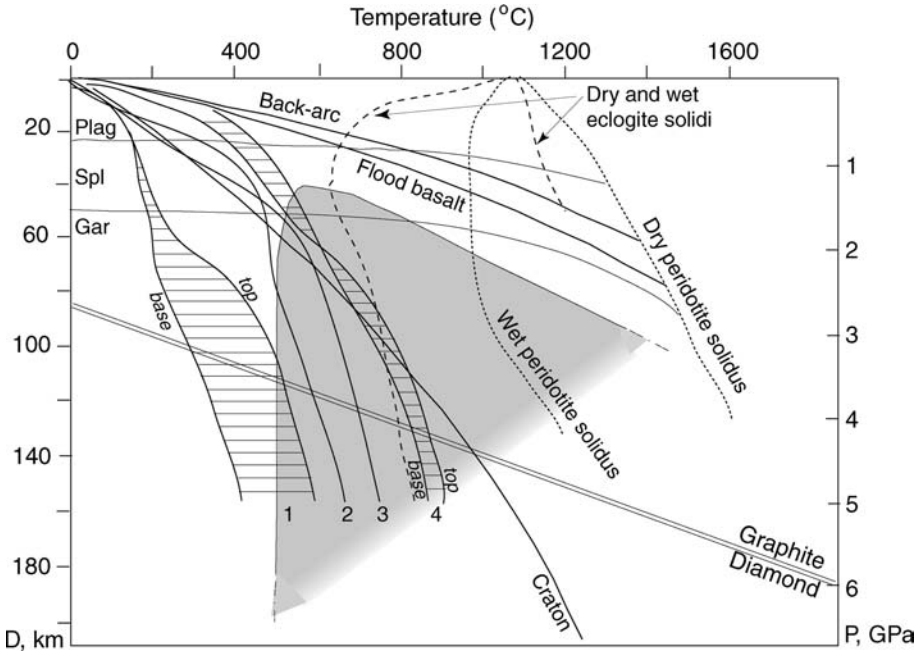

Fig. 7 Pressure–temperature diagram illustrating different thermal regimes, solidi and mineral stability fields of peridotite and eclogite. Transient geotherms 1–4 are estimated temperatures in subducted slabs: *1* old and fast (9 cm year^{-1}) subduction zone in NE Japan arc (Stern 2002); *2* modeled minimum temperatures in the 40 km thick slab subducting below the 67 km thick fixed plate with a convergence rate of 50 km per million years (Eberle et al. 2002); *3* model *T* profile along the top of the slab with 30° dip, 10 cm year^{-1} subduction rate, 100 km thickness of the slab, and 60 km thickness of the overriding plate (England and Wilkins 2004); *4* young and slow (4.5 cm year^{-1}) subduction zone in SW Japan arc (Stern 2002). Stippled fields in geotherms 1 and 4 encompass all possible slab temperatures between top and bottom of the slabs. The "Flood basalt" geotherm is based on a typical heat flow of 97 mW m^{-2} in areas of Cenozoic igneous activity (Pollack et al. 1993). The "Back-arc" geotherm is based on a regional value of 120 mW m^{-2} in a modern back-arc Tyrrhenian Sea with an active tholeiitic and calc-alkaline magmatism (Zito et al. 2003). The cratonic geotherm is a 40 mWt m^{-2} model continental geotherm of Pollack and Chapman (1977). Anhydrous and H_2O-saturated eclogite solidi and *P–T* conditions of the eclogite metamorphic facies (gray field) are from Stern 2002. Anhydrous and H_2O-saturated peridotite solidi and depth facies of peridotite (plagioclase, spinel, and garnet) are from Ulmer (2001). Graphite–diamond equilibrium is from Kennedy and Kennedy (1976)

temperatures. Based on this evidence, a xenocrystal origin is preferred for the Wawa diamonds.

A case for cratonic origin of Wawa diamonds

The Wawa diamonds may be xenocrystal cratonic. They may have formed in the continental mantle below the MGB (Thurston 2002; Sage et al. 1996a, b) which was subsequently (at ~2.9–2.7 Ga) rifted and generated a flood basalt province with voluminous komatiite–basalt–rhyolite volcanism (Sage et al. 1996a, b). Diamondiferous lamprophyre magmas are broadly coeval with the late, 2.7 Ga bimodal cycle of the volcanism, predating to postdating it by 40 and 20 Ma, respectively.

Cratonic xenocrystal origin explains many characteristics of the diamonds, such as (1) the absence of skeletal and re-entrant diamonds; (2) the presence of highly and non-uniformly resorbed and etched diamonds; (3) low nitrogen contents; (4) the presence of undeformed diamonds with highly aggregated nitrogen which formed at high (1,050–1,150°C) ambient mantle temperatures at depths greater than 160 km in the cold cratonic mantle (Fig. 7). In the cratonic model, disequilibrium assemblages of inclusions and rare CL colors of diamonds would be ascribed to effects of late metasomatic and metamorphic processes.

A cratonic origin for one of the other diamond suites found in the Wawa area (Cristal location) is advocated by Stachel et al. (2004). Such an origin is suggested by great (at least 250 km) depths of diamond formation, which, in turn, are indicated by inclusions of majorite and high (~1,250°C) mantle storage temperatures calculated from nitrogen aggregation states.

The cratonic model is difficult to reconcile with the formation depth of the host lamprophyres and their age. It was shown (Williams 2002) that Wawa lamprophyric magmas formed at 30–50 km depths, much shallower than the diamond stability field (Fig. 7). The relatively low Ti/Y ratio (<500) of the lamprophyres and unfractionated HREEs can be in equilibrium only with spinel peridotite, whereas deeper-seated kimberlite and lamproite magmas equilibrate in the garnet facies and have Ti/Y ratio >500 (Williams 2002). Thus, the diamonds cannot be entrained by Wawa lamprophyric magmas on their ascent to the surface in the cratonic mantle. Furthermore, the diamonds must have been removed from the deep mantle prior to rifting and

magmatism 2.9–2.7 Ga. In active flood basalt provinces with hot upwelling asthenosphere, shallow melting (Fig. 7) would destroy diamondiferous mantle roots of the continents (Helmsteadt and Gurney 1994).

A case for orogenic origin of Wawa diamonds

The alternative origin of the suite as orogenic xenocrystal diamonds is also possible. Wawa diamonds have the following characteristics common to orogenic diamonds: (1) a crystal size distribution significantly skewed towards microdiamonds; (2) the weak resorption (class 4 and 5) of the majority of diamonds; (3) CL spectra of yellow and green CL diamonds similar to that of orogenic microdiamonds; (4) an association with plagioclase and assemblages with metastable phases.

Within the convergent margin setting, the subducted slab remains the only cold block favorable for diamond crystallization and storage. Mantle segments below other terranes of the convergent margin such as the back-arc, or the mantle wedge (T∼1,400°C) are too hot to contain diamonds (Fig. 7). In the slab, on the contrary, diamond is stable at even shallower depths than those usually associated with cratonic diamonds. Diamond in the subducting slabs can form at 100–130 km depths, depending on subduction parameters and primarily on the rate of subduction (Fig. 7). These depths would not be different in the Archean, as ultrafast rates of subduction (Staudigel and King 1992) counterbalance the increased temperatures of hotter and shallower dipping slabs (e.g. Foley et al. 2003). The paradox of shallow Wawa lamprophyres and deep diamonds are reconciled with "cold plumes" (Gerya and Yuen 2003). The diamonds, in a complex mixture of different compositional blocks, could be carried up by fast "cold" plumes before being entrained by lamprophyres. Because the diamonds grew in a different way from "regular" cratonic diamonds, they acquired distinctive CL colors and mixed inclusion parageneses.

The major failure of the orogenic model is its inability to explain the presence of undeformed diamonds with highly aggregated nitrogen, formed at high ambient mantle temperatures. If we assume that the convergent regime existed in Wawa from 2.9 to 2.7 Ga as manifested by the MGB volcanism, then the diamonds had to reside at T = 1,140–1,390°C to produce the observed N aggregation state. These temperatures are unrealistically high for a slab (Fig. 7). Some other physical and chemical properties of the diamonds (low N, the presence of highly and non-uniformly resorbed diamonds) also do not agree with their possible orogenic origin.

Acknowledgements We are grateful to Band-Ore Resources Ltd. for their support and financial contribution to the project. This research was partly funded by a National Science and Engineering Research Grant and NSERC Industrial Post-Graduate Scholarship to N. Lefebvre. We are indebted to H. Grutter for his tremendous foresight and help in pursuing this exciting project. We wish to thank K. Breitsprecher for discussions and comments and R. Davies and R. Kerrich for helpful reviews.

References

Arias ZG, Helmstaedt H (1990) Structural evolution of the Michipicoten (Wawa) greenstone belt. Superior Province: evidence for an Archean fold and thrust belt. Geoscience Research Program, Summary of Research, 1989–1990. Ontario Geological Survey, Miscellaneous Paper 15, pp 107–114

Ayer JC, Amelin Y, Corfu F, Kamo S, Ketchum J, Kwok K, Trowell N (2002) Evolution of the southern Abitibi greenstone belt based on U–Pb geochronology: autochthonous volcanic construction followed by plutonism, regional deformation and sedimentation. Precambrian Res 115:63–95

Ayer JA, Conceicao RV, Ketchum JWF, Sage RP, Semenyna L, Wyman, DA (2003) The timing and petrogenesis of diamondiferous lamprophyres in the Michipicoten and Abitibi Greenstone belts. Summary of field work and other activities 2003, Ontario Geological Survey, Open File Report 6120, pp 10-1–10-9

Barrie CT (1990) U–Pb garnet and titanite age for the Bristol Township lamprophyre suite, western Abitibi Subprovince, Canada. Can J Earth Sci 27:1451–1456

Barron LM, Lishmund SR, Oakes GM, Barron BJ, Sutherland FL (1996) Subduction model for the origin of some diamonds in the Phanerozoic of eastern New South Wales. Aust J Earth Sci 43:257–267

Boyd FR (1989) Compositional distinction between oceanic and cratonic lithosphere. Earth Planet Sci Lett 96:15–26

Boyd SR, Kiflawi I, Woods GS (1994) The relationship between infrared absorption and the A defect concentration in diamond. Philos Mag B69:1149–1153

Boyd SR, Kiflawi I, Woods GS (1995) Infrared absorption by the nitrogen aggregate in diamond. Philos Mag B72:351–361

Buckle J (2002) The Wawa diamond enigma. CIM Bull 1061:85–87

Bulanova GP (1995) The formation of diamond. J Geochem Explor 53:1–23

Calvert AJ, Ludden JN (1999) Archean continental assembly in the southeastern Superior Province of Canada. Tectonics 18:412–429

Calvert AJ, Sawyer EW, Davis WJ, Ludden JN (1995) Archaean subduction inferred from seismic images of a mantle suture in the Superior Province. Nature 375:670–674

Capdevila R, Arndt N, Letendre J, Sauvage J-F (1999) Diamonds in volcaniclastic komatiite from French Guiana. Nature 399:456–458

Card KD, Ciesielski A (1986) Subdivisions of the Superior Province of the Canadian Shield. Geosci Can 13:5–13

Cartigny P, De Corte K, Shatsky VS, Ader M, De Paepe P, Sobolev NV, Javoy M (2001) The origin and formation of metamorphic microdiamonds from the Kokchetav massif, Kazakhstan: a nitrogen and carbon isotopic study. Chem Geol 176:265–281

Cartigny P, Chinn I, Viljoen KS, Robinson D (2004) Early Proterozoic ultrahigh pressure metamorphism: evidence from microdiamonds. Science 304:853–855

Chopin C (2003) Ultrahigh-pressure metamorphism: tracing continental crust into the mantle. Earth Planet Sci Lett 212:1–14

Clark CD, Collins AT, Woods GS (1992) Optical spectroscopy of diamond. In: Field JE (ed) The properties of natural and synthetic diamond. Academic, New York, pp 35–69

Collins AT (1992) The characterization of point defects in diamond by luminescence spectroscopy. Diam Relat Mater 1:1457–1469

De Corte K, Cartigny P, Shatsky VS, De Paepe P, Sobolev NV, Javoy M (1999) Characteristics of microdiamonds from UHPM rocks of the Kotchetav massif. In: Gurney JJ, Gurney JL, Pascoe MD, Richardson SH (eds) Proceedings of the 7th international kimberlite conference, Red Roof Design, Cape Town, pp 164–173

Eberle MA, Grasset O, Sotin C (2002) A numerical study of the interaction between the mantle wedge, subducting slab, and overriding plate. Phys Earth Planet Interiors 134:191–202

England P, Wilkins C (2004) A simple analytical approximation to the temperature structure in subduction zones. Geophys J Int 159:1138–1154

Evans T (1992) Aggregation of nitrogen in diamonds. In: Field JE (ed) The properties of natural and synthetic diamond. Academic, New York, pp 259–290

Foley SF, Buhre S, Jacob DE (2003) Evolution of the Archean crust by delamination and shallow subduction. Nature 421:249–252

Gerya TV, Yuen DA (2003) Rayleigh–Taylor instabilities from hydration and melting propel "cold plumes" at subduction zones. Earth Planet Sci Lett 212:47–62

Graham RJ, Ravi KV (1992) Cathodoluminescence investigation of impurities and defects in single crystal diamond grown by the combustion-flame method. Appl Phys Lett 60:1310–1312

Griffin WL, O'Reilly SY, Davies RM (2000) Subduction-related diamond deposits? Constraints, possibilities and new data from Eastern Australia. In: Spry PG, Marshall B, Vokes FM (eds) Metamorphosed and metamorphogenic ore deposits, reviews in economic geology, 11. Society of Economic Geologists, Socorro, pp 291–310

Gurney JJ (1989) Diamonds. In: Ross J, Jacques AL, Ferguson J, Green DH, O' Reilly SY, Danchin RV, Janse AJA (eds) Kimberlites and related rocks, vol 2, no. 14. Blackwell, Carlton, pp 935–965

Hanley PL, Kiflawi I, Lang AR (1977) On topographically identifiable sources of cathodoluminescence in natural diamonds. Philos Trans R Soc Lond A284:329–368

Harris JW (1992) Diamond geology. In: Field JE (ed) The properties of natural and synthetic diamond. Academic, New York, pp 345–394

Hayashi K, Watanabe H, Yamanaka S, Okushi H, Kajimura K, Sekiguchi T (1996) Direct observation of hydrogen-related luminescent states in subsurface region of homoepitaxial diamond films. Appl Phys Lett 69:1122–1124

Heaman LM, Kjarsgaard BA, Creaser RA (2004) The temporal evolution of North American kimberlites. Lithos 76(1–4):377–397

Helmstaedt H, Gurney JJ (1994) Geotectonic controls on the formation of diamonds and their kimberlitic and lamproitic host rocks: applications to diamond exploration. In: Meyer HOA, Leonardos OH (eds) Proceedings of the 5th international kimberlite conference, Campanhia de Pesquia de Recrurso Minerais, Rio de Janeiro, vol 2, pp 51–68

Hoffman PF (1990) Geological constraints in the origin of the mantle beneath the Canadian Shield. Philos Trans R Soc Lond A331:523–532

Iakoubovskii K, Adriaenssens GJ (1999) Photoluminescence in CVD diamond films. Phys Status Solidi—Appl Res 172:123–129

Ishida H, Ogasawara Y, Ohsumi K, Saito A (2003) Two stage growth of microdiamond in UHP dolomite marble from Kokchetav massif, Kazakhstan. J Metamorph Geol 21:515–522

Kennedy CS, Kennedy GC (1976) The equilibrium boundary between graphite and diamond. J Geophys Res 81:2467–2470

Lefebvre N, Kopylova M, Kivi K (2005) Archean calc-alkaline lamprophyres of Wawa, Ontario, Canada: unconventional diamondiferous volcaniclastic rocks. Precambrian Res 138:57–87

Lindblom J, Holsa J, Papunen H, Hakkanen H, Mutanen J (2003) Differentiation of natural and synthetic gem-quality diamond by luminescence properties. Opt Mater 24:243–251

Magee CW, Taylor WR (1999) Constraints from luminescence on the history and origin of carbonado. In: Gurney JJ, Gurney JL, Pascoe MD, Richardson SH (eds) Proceedings of the 7th international kimberlite conference, Red Roof Design, Cape Town, pp 529–532

Marinelli M, Hatta A, Ito T, Hiraki A, Nishino T (1996) Band-A emission in synthetic diamond films: a systematic investigation. Appl Phys Lett 68:1631–1633

Martineau PM, Lawson SC, Taylor AJ, Quinn SJ, Evans DJF, Crowder MJ (2004) Identification of synthetic diamond grown using chemical vapor deposition (CVD). Gems Gemol 40:2–25

McCallum ME, Huntley PM, Falk RW, Otter ML (1994) Morphological, resorption and etch feature trends of diamonds from kimberlite populations within the Colorado-Wyoming state line district, USA. In: Meyer HOA, Leonardos O (eds) Proceedings of the 5th international kimberlite conference, Brasilia, Brazil, Companhia de Pesquisa de Recursos Minerals, pp 78–97

McNamara KM, Williams BE, Gleason KK (1997) Characterization methods. In: Prelas MA, Popovici G, Bigelow LK (eds) Handbook of industrial diamonds and diamond films. Marcel Dekker, New York, pp 413–480

Mendelssohn MJ, Milledge HJ (1995) Geologically significant information from routine analysis of the mid-infrared spectra of diamonds. Int Geol Rev 37:95–110

Milledge HJ, Woods PA, Beard AD, Shelkov D, Willis B (1999) Cathodoluminescence of polished carbonado. In: Gurney JJ, Gurney JL, Pascoe MD, Richardson SH (eds) Proceedings of the 7th international kimberlite conference, Red Roof Design, Cape Town, pp 589–590

Miller C, Thoni M (1997) Eo-Alpine eclogitisation of permian MORB-type gabbros in the Koralpe (Eastern Alps, Austria): new geochronological, geochemical and petrological data. Chem Geol 137:283–310

Ogasawara Y (2005) Microdiamonds in ultrahigh-pressure metamorphic rocks. Elements 1:91–96

Paczner G, Gaft M, Marfunin A (2000) Systems of interacting luminescence centers in natural diamonds: laser-induced time-resolved cathodoluminescence spectroscopy. In: Pagel M, Barbin V, Blanc P, Ohenstetter D (eds) Cathodoluminescence in geosciences. Springer, Berlin Heidelberg New York 514 pp

Pattison DRM, Levinson AA (1995) Are euhedral microdiamonds formed during ascent and decompression of kimberlite magma? Implications for use of microdiamonds in diamond grade estimation. Appl Geochem 10:725–738

Pearson DG, Canil D, Shirey SB (2002) Mantle samples included in volcanic rocks: xenoliths and diamonds. In: Carlson RW (ed) Treatise on geochemistry, vol 2. Elsevier, Amsterdam, pp 171–275

Polat A, Kerrich R (2001) Geodynamic processes, continental growth, and mantle evolution recorded in late Archean greenstone belts of the southern Superior Province. Canada. Precambrian Res 112(1–2):5–25

Pollack HN, Chapman DS (1977) On the regional variation of heat flow, geotherms, and lithospheric thickness. Tectonophysics 38:279–296

Pollack HN, Hurter SJ, Johnston JR (1993) Heat flow from the Earth's interior: analysis of the global data set. Rev Geophys 31(3):267–280

Robinson DN, Scott JA, Van Niekerk A, Anderson VG (1989) The sequence of events reflected in the diamonds of some southern African kimberlites. In: Ross J (ed) Kimberlites and related rocks. Volume 2: their mantle/crust setting, diamonds, and diamond exploration. Geological Society of Australia Special Publication 14. Blackwell, Victoria, pp 990–1000

Rock NMS (1991) Lamprophyres. Blackie, Glasgow, 286 pp

Rubatto D, Hermann J (2001) Exhumation as fast as subduction? Geology 29:3–6

Sage RP (1994) Geology of the Michipicoten Greenstone Belt. Ontario Geological Survey, Sudbury, Open file report 5888, 592 pp

Sage RP, Lightfoot PC, Doherty W (1996a) Bimodal cyclical Archean basalts and ryolites form the Michipicoten (Wawa) greenstone belt, Ontario: geochemical evidence for magma contributions from the asthenospheric mantle and ancient continental lithosphere near the southern margin of the Superior Province. Precambrian Res 76:119–153

Sage RP, Morris TF, Crabtree D, Murray CA, Bennett G, Hailstone M, Nicholson T, Pianosi S, Josey S (1996b) Ultramafic dike with mantle xenoliths; implications to diamond exploration in Wawa. In: Proceedings and abstracts—Institute on Lake Superior Geology meeting, vol 42, Part 1, 52 pp

Schertl HP, Okay AI (1994) A coesite inclusion in dolomite in Dabie-Shan, China—petrological and theological significance. Eur J Mineral 6:995–1000

Schulze DJ, Harte B, Valley JW, Channer DMD (2004) Evidence of subduction and crust–mantle mixing from a single diamond. Lithos 77:349–358

Smith D (1999) Temperatures and pressures of mineral equilibration in peridotite xenoliths: review, discussion, and implications. In: Fei Y, Bertka C, Mysen B (eds) Mantle petrology: field observations and high pressure experimentation: a tribute to Francis (Joe) Boyd. Geochemical Society Special Publication 6, pp 171–188

Sobolev NV, Shatsky VS (1990) Diamond inclusions in garnets from metamorphic rocks: a new environment of diamond formation. Nature 243:742–746

Sobolev VN, Taylor LA, Snyder GA, Sovolev NV, Pokhilenko NP, Kharkiv AD (1997) A unique metasomatized peridotite xenolith from the Mir kimberlite pipe (Yakutia). In: Proceedings of the 6th international kimberlite conference, Geologiya I Geofizika, 38, 1, pp 206–215

Stachel T, Harris JW (1997) Syngenetic inclusions in diamond from the Birim field (Ghana)—a deep peridotitic profile with a history of depletion and re-enrichment. Contrib Mineral Petrol 127:336–352

Stachel T, Brey GP, Harris JW (2000) Kankan diamonds (Guinea) I: from the lithosphere down to the transition zone. Contrib Mineral Petrol 140:1–15

Stachel T, Harris JW, Aulbach S, Deines P (2002) Kankan diamonds (Guinea) III; delta (super 13) C and nitrogen characteristics of deep diamonds. Contrib Mineral Petrol 142:465–475

Stachel T, Blackburn L, Kurszlaukis S, Barton E, Walker EC (2004) Diamonds from the Cristal and Genesis volcanics, Wawa area, Ontario. In: 32nd annual Yellowknife Geoscience forum, pp 74–75

Staudigel H, King CD (1992) Ultrafast subduction: the key to slab recycling efficiency and mantle differentiation? Earth Planet Sci Lett 109:517–530

Stern RJ (2002) Subduction zones. Rev Geophys 40(4):3–38

Stern RA, Hanson GN (1992) Marathon dykes: Rb–Sr and K–Ar geochronology of ultrabasic lamprophyres from the vicinity of McKillar Harbour, northwestern Ontario, Canada. Can J Earth Sci 20:193–227

Stockhert B, Duyster J, Trepmann C, Masonne HJ (2001) Microdiamond daughter crystals precipitated from supercritical COH + silicate fluids included in garnet, Erzgebirge, Germany. Geology 29:391–394

Stott GM (1997) The Superior Province, Canada Greenstone Belts. In: De Wit M, Ashwal L (eds) Oxford monograph on geology and geophysics 35. Oxford University Press, New York pp 480–507

Stott GM, Ayer JA, Wilson AC, Grabowski GPB (2002) Are the Neoarchean diamond-bearing breccias in the Wawa area related to late-orogenic alkalic and "sanukitoid" intrusions? Summary of field work and other activities 2002, Ontario Geological Survey, Open file report 6100, pp 9-1-9-10

Sylvester PJ, Attoh K, Schulz KJ (1987) Tectonic setting of late Archean bimodal volcanism in the Michipicoten (Wawa) greenstone belt, Ontario. Can J Earth Sci 24:1120–1134

Takeuchi D, Watanabe K, Yamanaka S, Okushi H (2001) Origin of band-A emission in diamond thin films. Phys Rev B 63:245328-1–245328-7

Taylor WR, Jacques AL, Ridd M (1990) Nitrogen-defect aggregation characteristics of some Australian diamonds: time–temperature constraints on the source region of pipe and alluvial diamonds. Am Mineral 75:1290–1310

Thurston PC (2002) Autochthonous development of Superior Province greenstone belts? Precambrian Res 115:11–36

Turek A, Sage RP, Van Schumus WR (1992) Advances in the U–Pb zircon geochronology on the Michipicoten Greenstone Belt, Superior Province, Ontario, Canada. Can J Earth Sci 29:1154–1165

Ulmer P (2001) Partial melting in the mantle wedge—the role of H_2O in the genesis of mantle-derived "arc-related" magma. Phys Earth Planet Interiors 127:215–232

Vance ER, Milledge HJ (1972) Natural and laboratory alpha-particle irradiation of diamond. Mineral Mag 38:878–885

Viljoen KS, Phillips D, Harris JW, Robinson DN (1999) Mineral inclusions in diamonds from the Venetia kimberlites, Northern Province, South Africa. In: Gurney JJ, Gurney JL, Pascoe MD, Richardson SH (eds) Proceedings of the 7th international kimberlite conference, Red Roof Design, Cape Town, pp 888-895

Williams F (2002) Diamonds in late Archean calc-alkaline lamprophyres, Ontario, Canada: origins and implications. BSc (Honours) Thesis, University of Sydney, Sydney, Australia, 85 pp

Williams HR, Stott GM, Heather KB, Muir TL, Sage RP (1991) Wawa Subprovince. In: Thurston PC, Williams HR, Sutcliffe RH, Stott GM (eds) Geology of Ontario, special vol 4(1). Ministry of Northern Development and Mines, Ontario Geological Survey, Sudbury, pp 485–538

Woods GS (1986) Platelets and the infrared absorption of type Ia diamonds. Proc R Soc Lond A407:219–238

Wyman D, Kerrich R (1989) Archean lamprophyre dikes of the Superior province, Canada: distribution, petrology and geochemical characteristics. J Geophys Res 94(B4):4667–4696

Wyman D, Kerrich R (1993) Archean shoshonitic lamprophyres of the Abitibi Subprovince, Canada: petrogenesis, age, and tectonic setting. J Petrol 34:1067–1109

Wyman D, Kerrich R (2002) Assembly of Archean cratonic mantle lithosphere and crust: plum–arch interaction in the Abitibi-Wawa subduction–accretion complex. Precambrian Res 115:37–62

Yang X, Barnes AV, Albert MM, Albridge JT, McKinley JT, Tolk NH, Davidson JL (1995) Cathodoluminescence and photoluminescence of chemical-vapor-deposited diamond. J Appl Phys 77:1758–1761

Yoshioka N, Ogasawara Y (2005) Cathodoluminescence of microdiamond in dolomite marble from the Kokchtav Massif—another evidence for two-stage growth of diamond. Int Geol Rev (in press)

Zaitsev A (2001) Optical properties of diamond; a data handbook. Springer, Berlin Heidelberg New York, 502 pp

Zito G, Mongelli F, De Lorenzo S, Doglioni C (2003) Heat flow and geodynamics in the Tyrrhenian Sea. Terra Nova 15:425–432